Controllable persistent luminescence in bismuth activated memory phosphors by trap management for artificial intelligence anti-counterfeiting

Dangli Gao,*[ab] Chengxue Du,[a] Yuqiang Wang,[b] Wenqian Xu,[b] Wenna Gao,[b] Qing Pang,[b] and Yuhua Wang*[c]

[a] School of Environmental and Municipal Engineering, Xi'an University of Architecture and Technology, Xi'an, Shaanxi 710055, China

[b] College of Science, Xi'an University of Architecture and Technology, Xi'an, Shaanxi 710055, China. E-mail: gaodangli@163.com, gaodangli@xauat.edu.cn

[c] National and Local Joint Engineering Laboratory for Optical Conversion Materials and Technology of National Development and Reform Commission, School of Materials and Energy, Lanzhou University, Lanzhou 730000, Gansu, China. E-mail: wyh@lzu.edu.cn

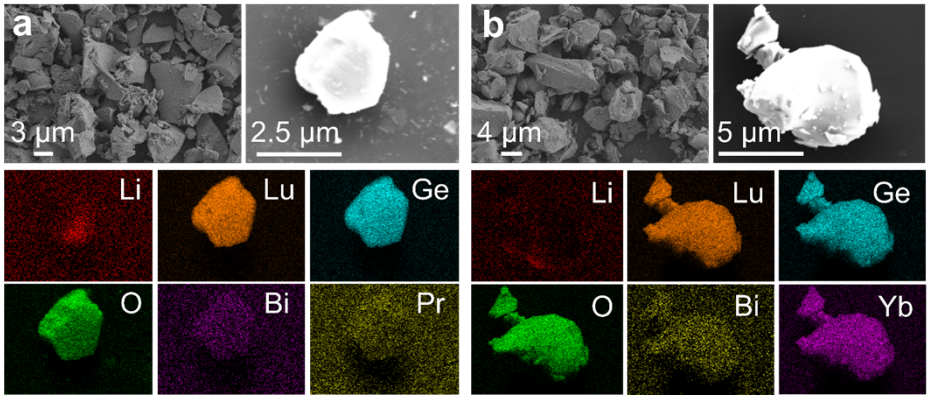

Fig. S1. SEM images and elemental mappings of (a) LLGO:Bi,Pr and (b) LLGO:Bi,Yb phosphors.

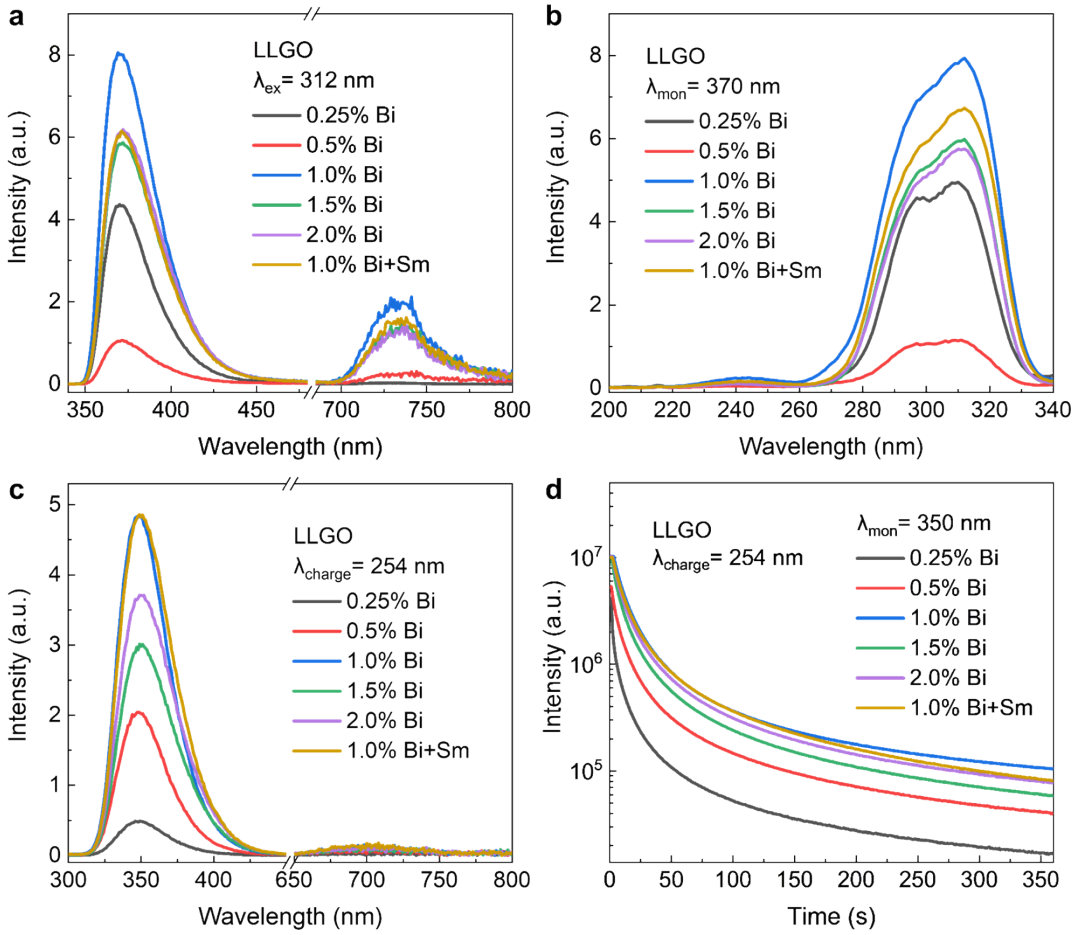

Fig. S2. The effect of Bi^{3+} doping concentration or trace doping Sm^{3+} (10^{-7} mmol) on the luminescence characteristics of LLGO:Bi phosphors. (a) PL spectra, (b) PLE spectra, (c) PersL spectra, and (d) PersL decay curves.

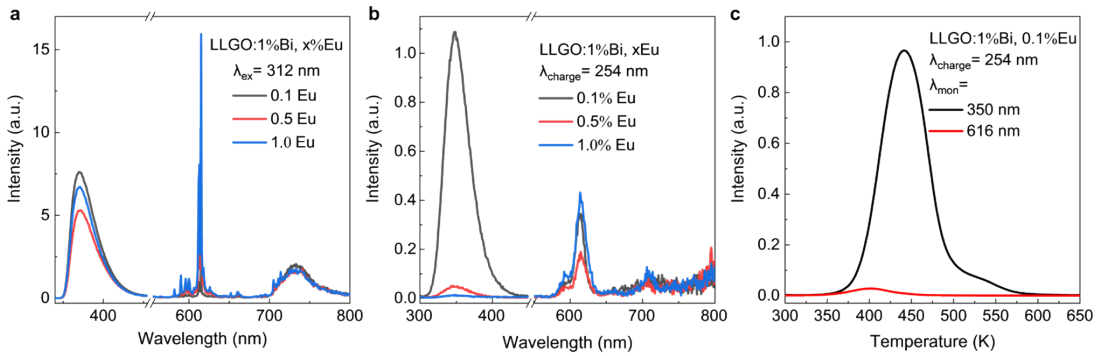

Fig. S3. The effect of Eu^{3+} doping concentration on the luminescence characteristics of LLGO:Bi phosphors. (a) PL spectra, (b) PersL spectra, and (c) TL spectra.

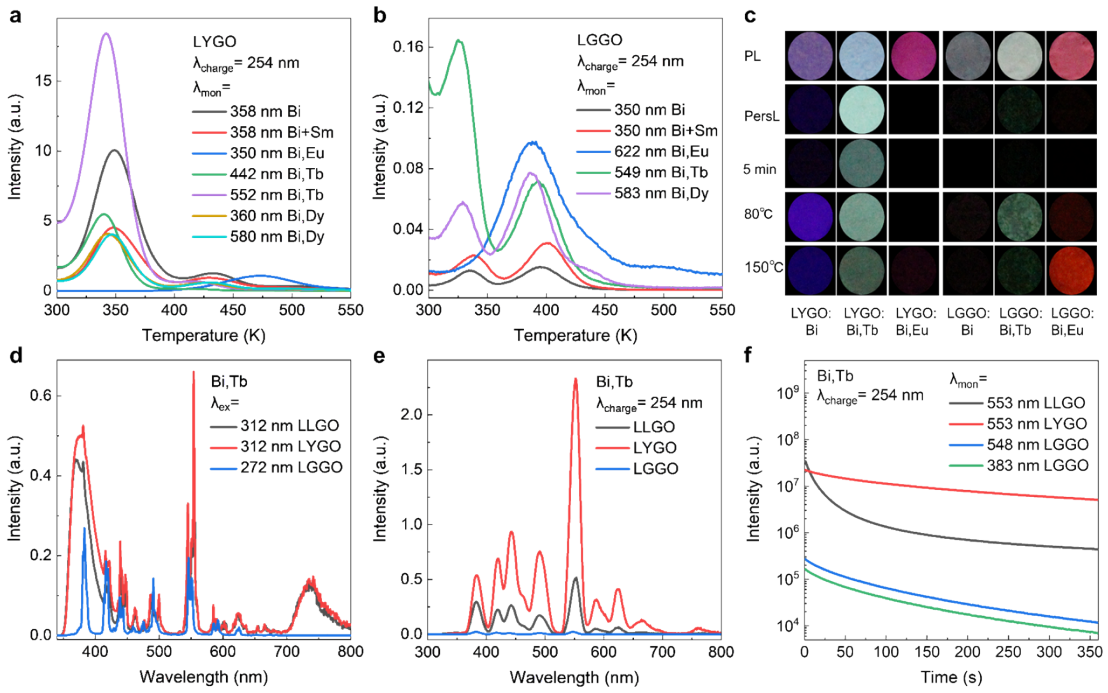

Fig. S4. The effect of matrix lattice and Ln^{3+} doping on the fluorescence characteristics of Bi doped germanate based phosphors. (a,b) TL spectra of LYGO/LGGO:Bi,Ln (Ln=Eu, Tb, Dy, and trace Sm). (c) Comparison of multimode fluorescence photos of LYGO/LGGO:Bi,Ln phosphors. (d-f) The comparison of PL, PersL spectra and PersL decay curves of LLGO:Bi,Tb, LYGO:Bi,Tb and LGGO:Bi,Tb samples.

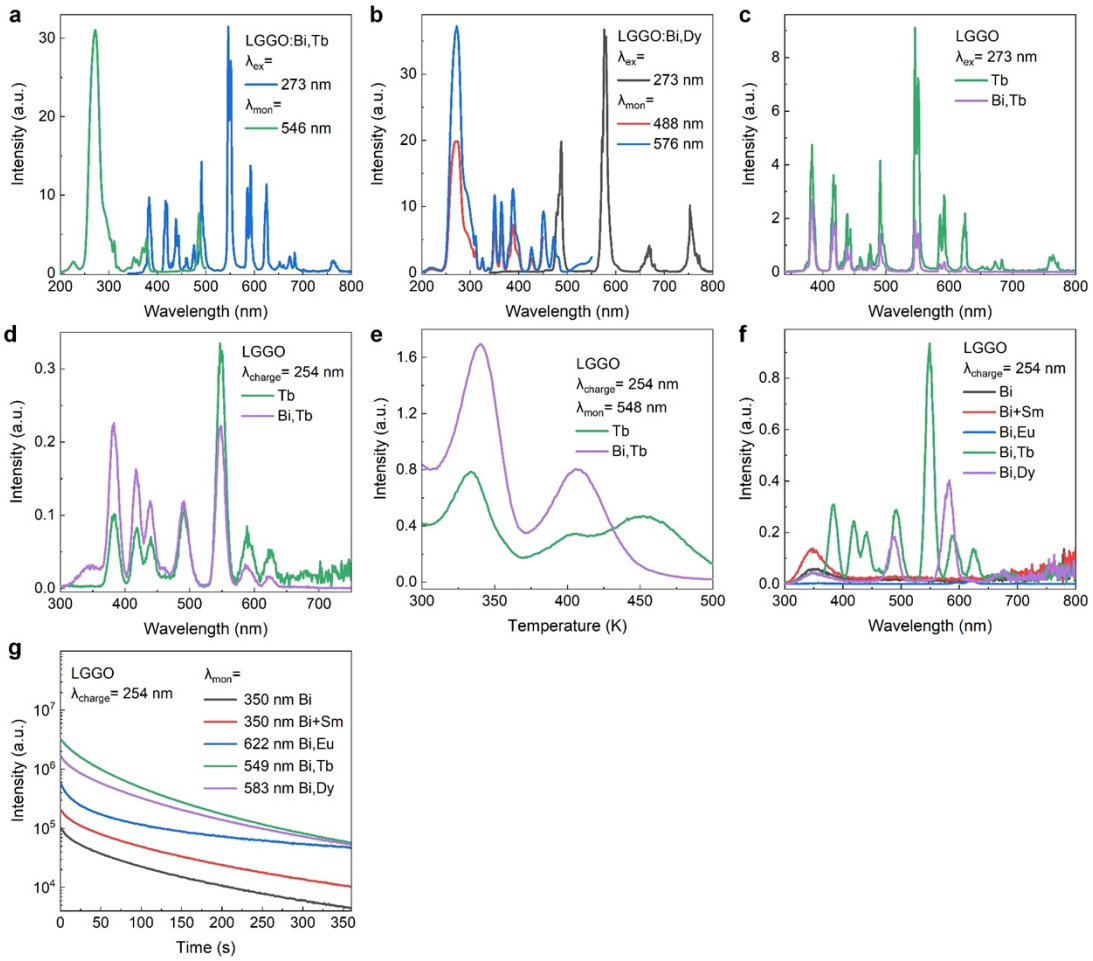

Fig. S5. The effect of Ln^{3+} (Ln=Eu, Tb, Dy and trace Sm) doping on the luminescence characteristics of LGGO:Bi phosphors. (a,b) PLE and PL spectra of LGGO:Bi,Tb and LGGO:Bi,Dy, respectively. (c) Comparison of PL spectra of LGGO:Bi,Tb and LGGO:Tb. (d) Comparison of PersL spectra of LGGO:Bi,Tb and LGGO:Tb. (e) Comparison of TL spectra of LGGO:Bi,Tb and LGGO:Tb. (f,g) Comparison of PersL spectra and PersL decay curves of LGGO:Bi,Ln (Ln=Eu, trace Sm, Tb and Dy) phosphors, respectively.

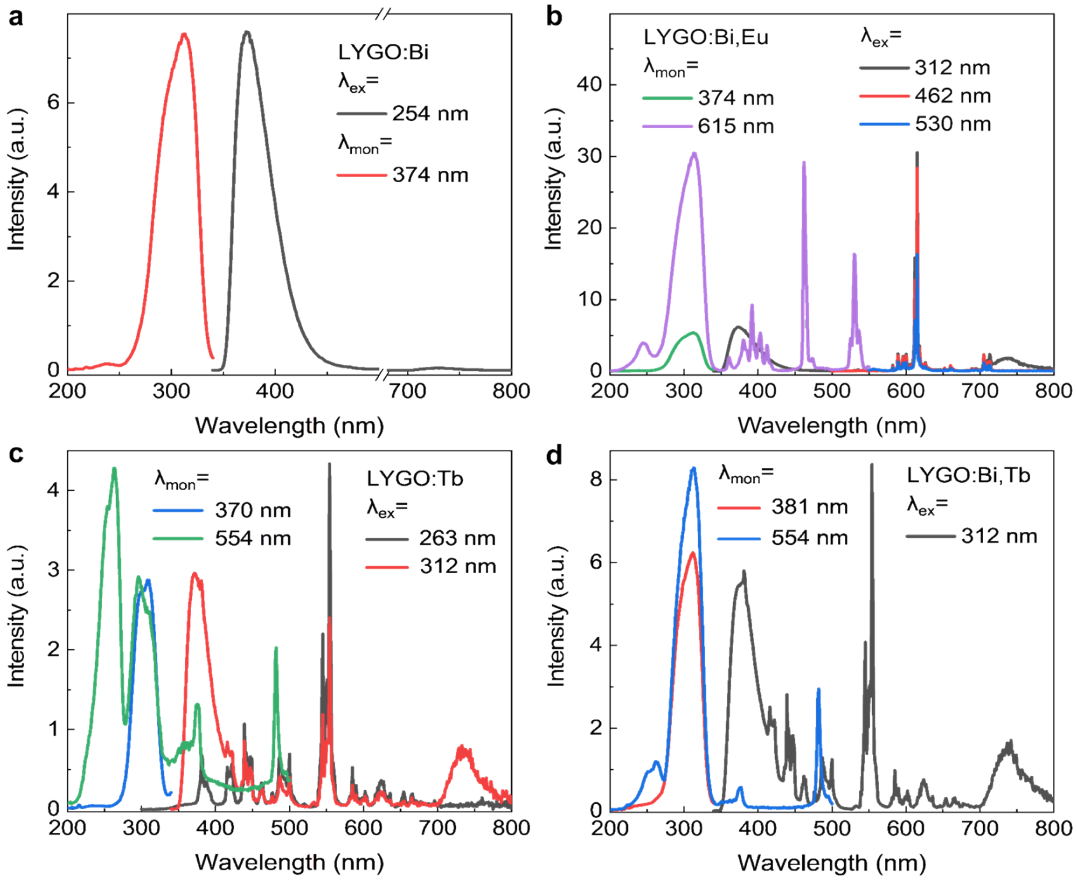

Fig. S6. The effect of Ln^{3+} (Ln=Eu and Tb) doping on the luminescence characteristics of LYGO:Bi phosphors. (a,b) PLE and PL spectra of LYGO:Bi and LYGO:Bi,Eu, respectively. (c,d) PLE and PL spectra of LYGO:Tb and LYGO:Bi,Tb, respectively.

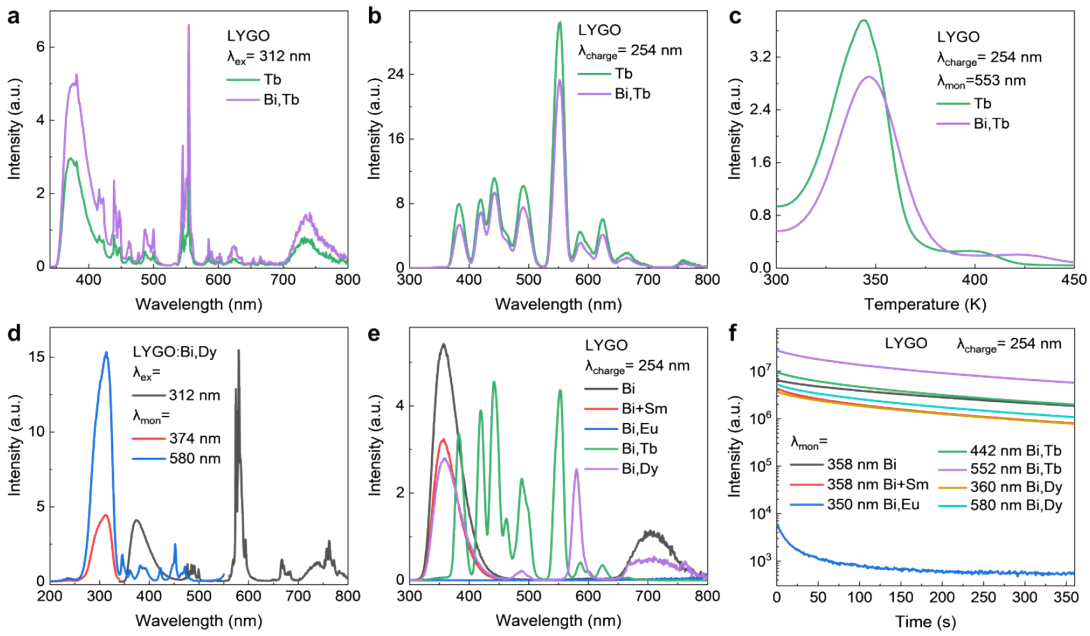

Fig. S7. The effect of Ln^{3+} doping on the luminescence characteristics of LYGO:Bi phosphors. (a-c) PL, PersL and TL spectra of LYGO:Tb and LYGO:Bi,Tb, respectively. (d) PLE and PL spectra of LYGO:Bi,Dy. (e,f) Comparison of PersL spectra and PersL decay curves of LYGO:Bi,Ln (Ln=Eu, trace Sm, Tb and Dy).

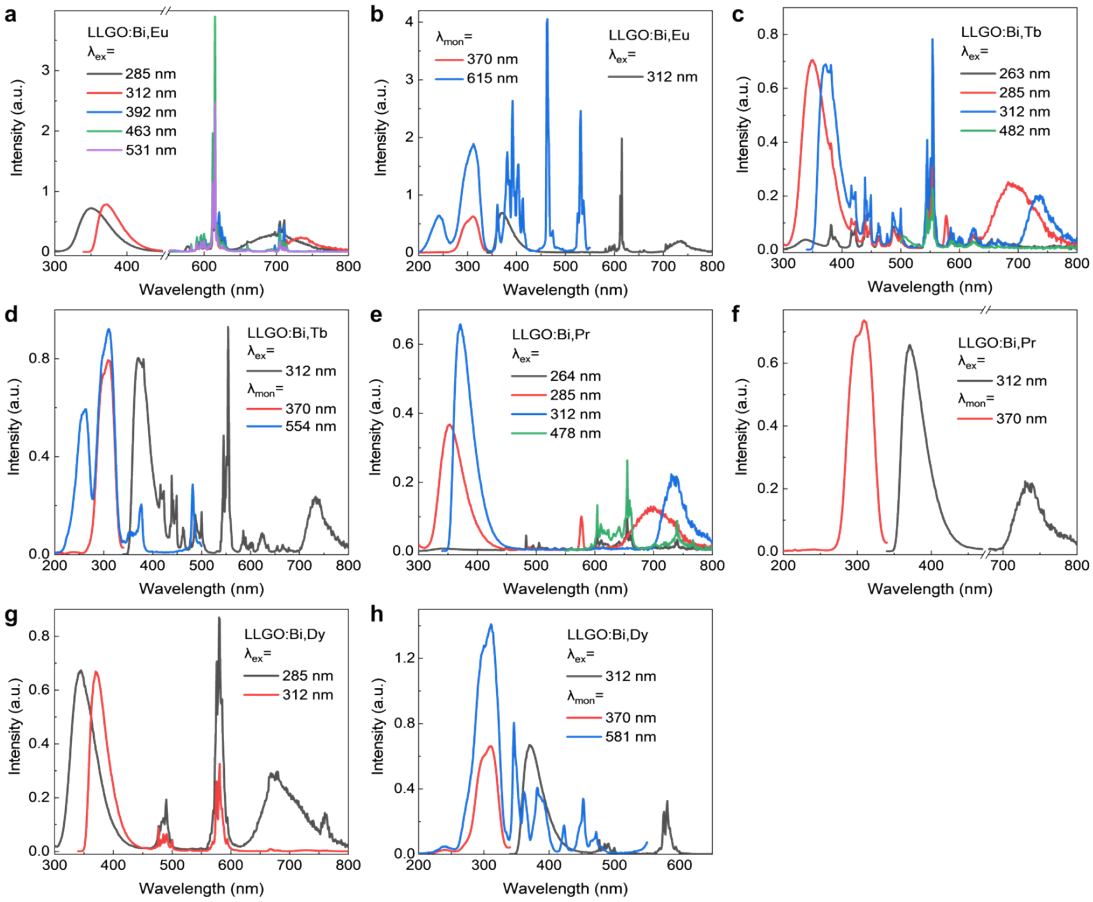

Fig. S8. The effect of Ln^{3+} (Ln=Eu, Tb, Pr and Dy) doping on the luminescence characteristics of LLGO:Bi phosphors. (a) PL spectra of LLGO:Bi,Eu under selective excitation. (b) Comparison of PLE and PL spectra of LLGO:Bi,Eu. (c) PL spectra of LLGO:Bi,Tb under selective excitation. (d) Comparison of PLE and PL spectra of LLGO:Bi,Tb. (e) PL spectra of LLGO:Bi,Pr under selective excitation. (f) PLE and PL spectra of LLGO:Bi,Pr. (g) PL spectra of LLGO:Bi,Dy under selective excitation. (h) PLE and PL spectra of LLGO:Bi,Dy.

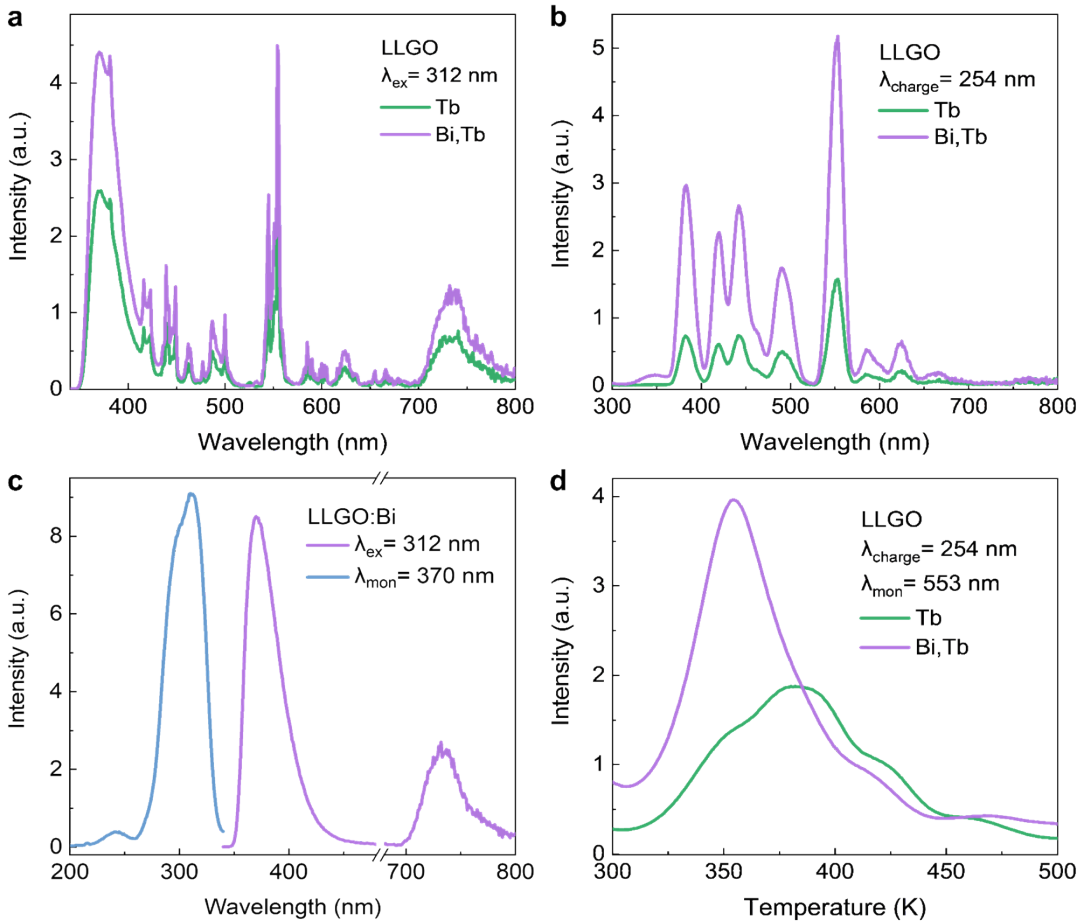

Fig. S9. The comparison of fluorescence characteristics for LLGO:Tb and LLGO:Bi,Tb phosphors. (a,b) PL and PersL spectra of LLGO:Bi,Tb and LLGO:Tb. (c) PL and PLE spectra of LLGO:Bi. (d) TL spectra of LLGO:Bi,Tb and LLGO:Tb.

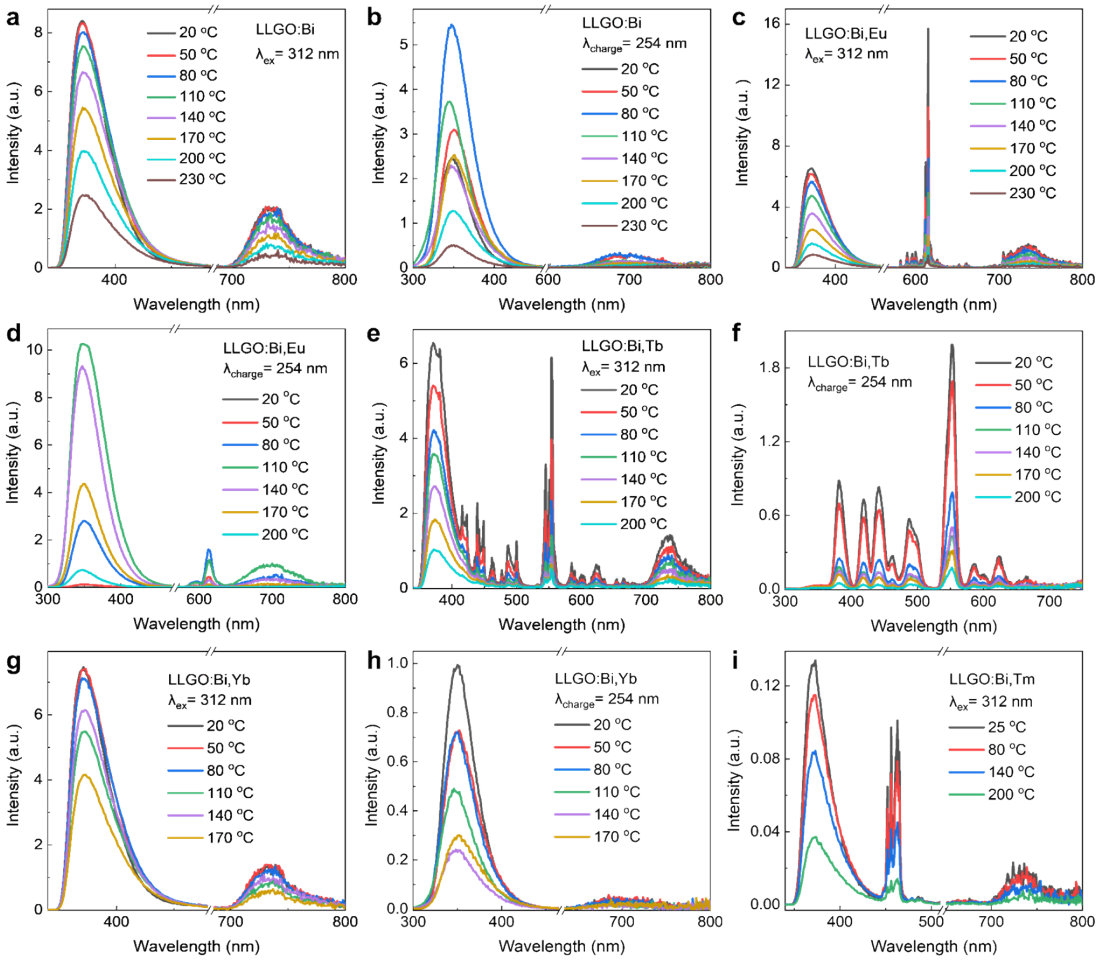

Fig. S10. The effect of temperature on the fluorescence characteristics of LLGO:Bi,Ln (Ln=Eu, Tb and Yb) phosphors, with the spectra of LLGO:Bi phosphor as a reference. Temperature-dependent PL and PersL spectra of LLGO:Bi (a,b), LLGO:Bi,Eu (c,d), LLGO:Bi,Tb (e,f), and LLGO:Bi,Yb (g,h). (i) Temperature-dependent PL spectra of LLGO:Bi,Tm.

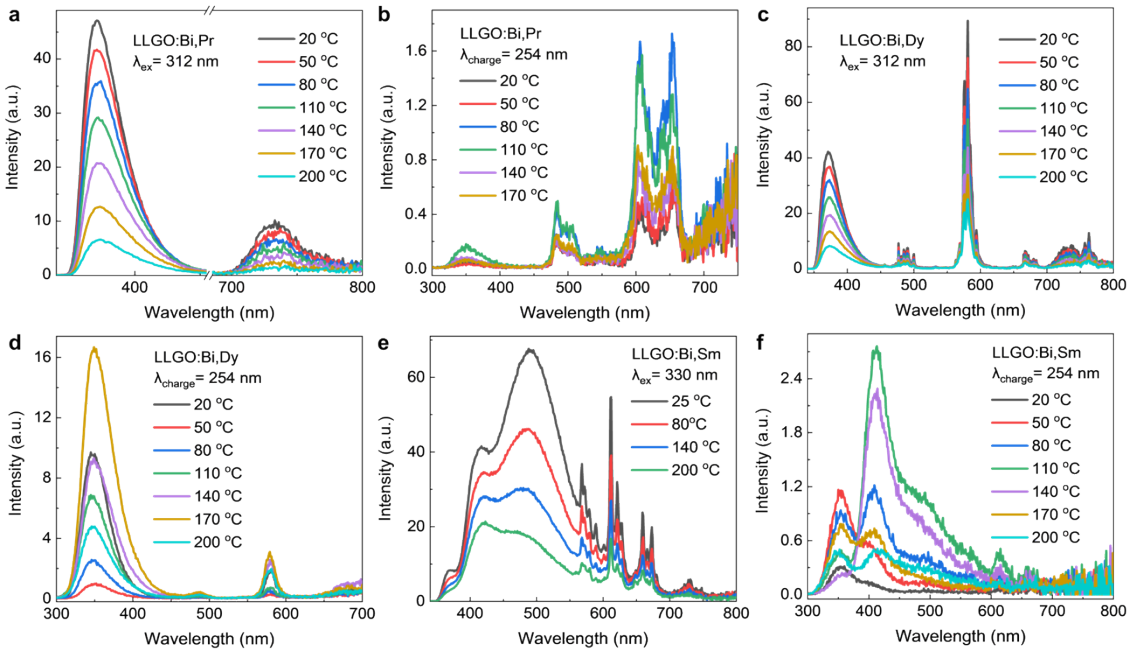

Fig. S11. The effect of temperature on the fluorescence characteristics of LLGO:Bi,Ln (Ln=Pr, Dy and Sm) phosphors, with the spectra of LLGO:Bi phosphor as reference. Temperature-dependent PL and PersL spectra of LLGO:Bi,Pr (a,b), LLGO:Bi,Dy (c,d), and LLGO:Bi,Sm (e,f).

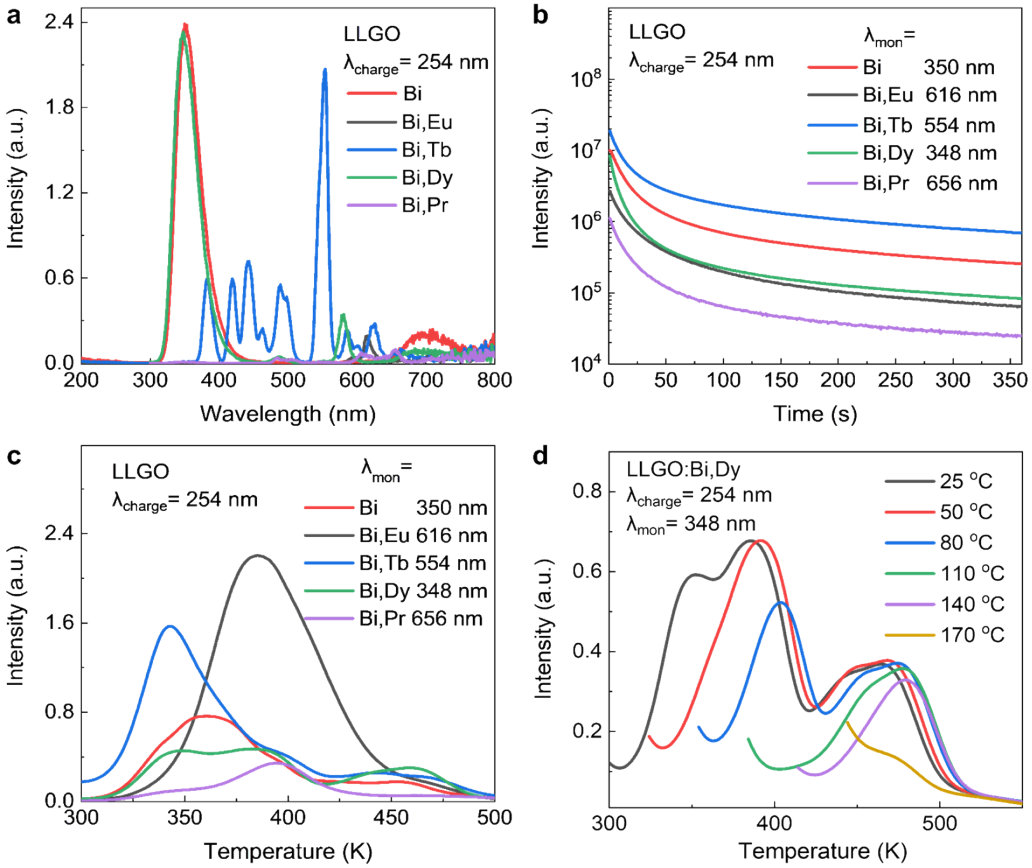

Fig. S12. Comparison of afterglow characteristics and TL curves characteristics of LLGO:Bi,Ln phosphors. (a-c) PersL, PersL decay curves and TL spectra of LLGO:Bi,Ln (Ln=Eu, Tb, Dy and Pr). (d) Temperature-dependent TL spectra of LLGO:Bi,Dy.

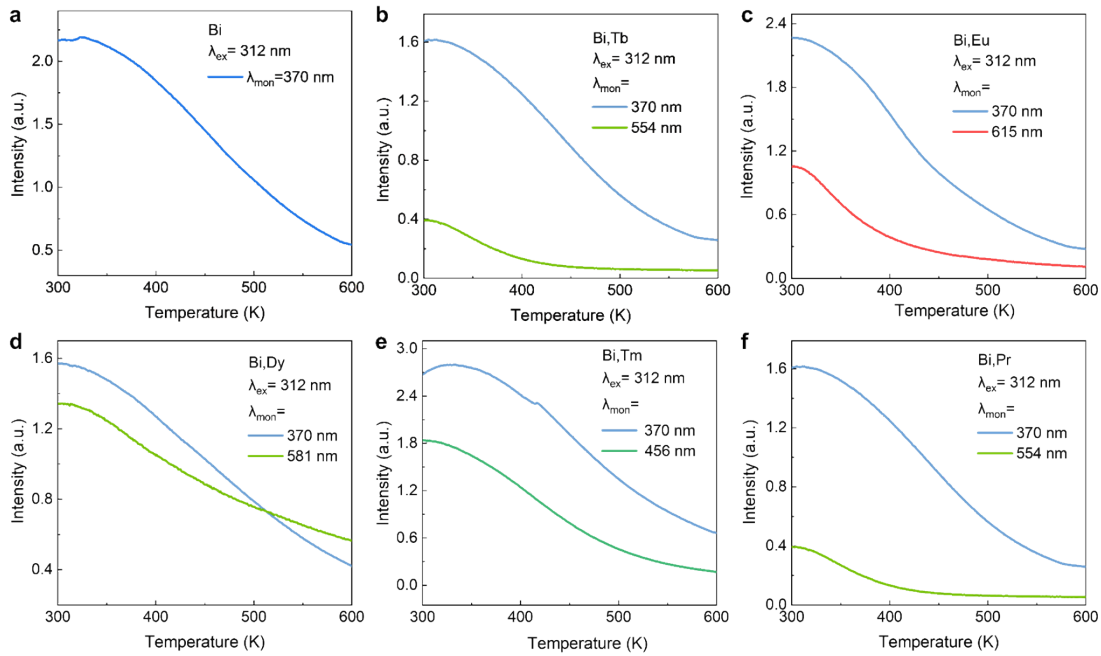

Fig. S13. Temperature-dependent PL intensity as a function of temperature of LLGO:Bi,Ln (Ln=Eu, Tb, Dy, Tm and Pr) phosphors. (a) LLGO:Bi, (b) LLGO:Bi,Tb, (c) LLGO:Bi,Eu, (d) LLGO:Bi,Dy, (e) LLGO:Bi,Tm, and (f) LLGO:Bi,Pr.

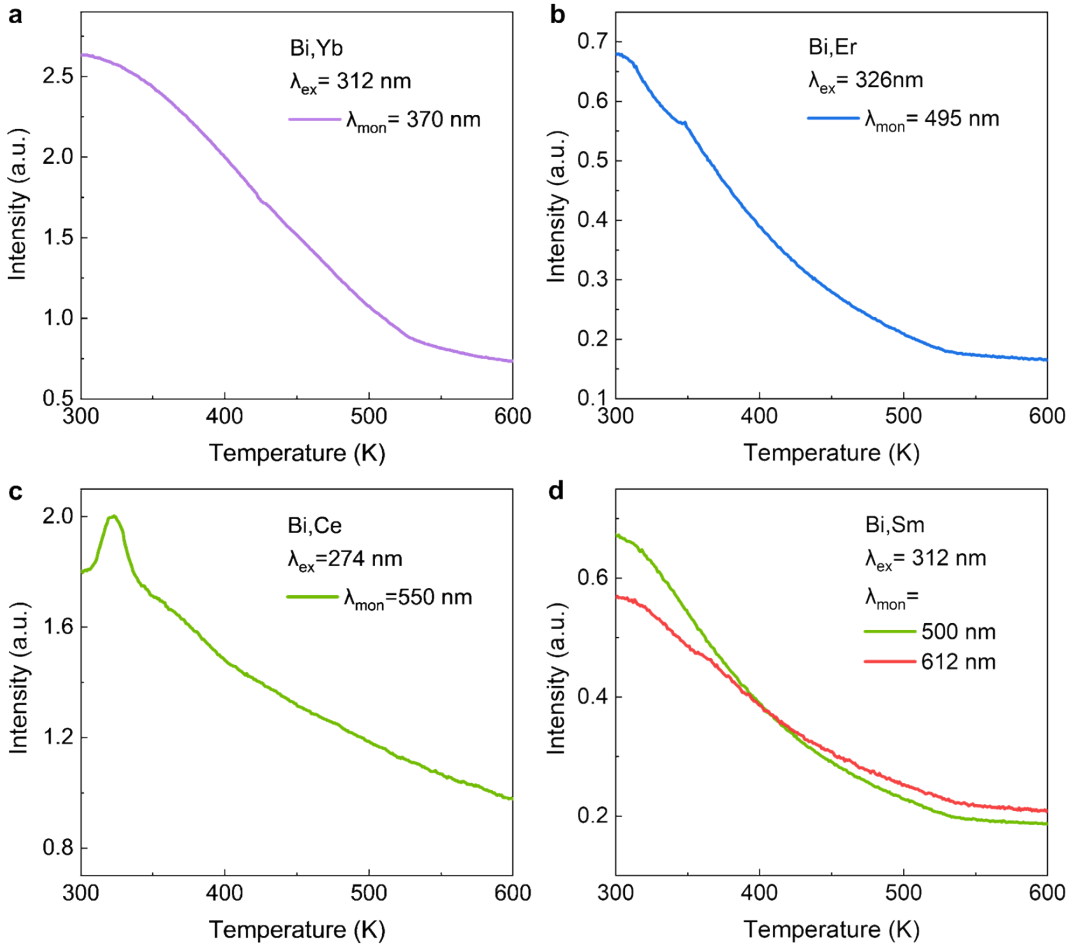

Fig. S14. Temperature-dependent PL intensity as a function of temperature of LLGO:Bi,Ln (Ln=Yb, Er, Ce and Sm) phosphors. (a) LLGO:Bi,Yb, (b) LLGO:Bi,Er, (c) LLGO:Bi,Ce, and (d) LLGO:Bi,Sm.

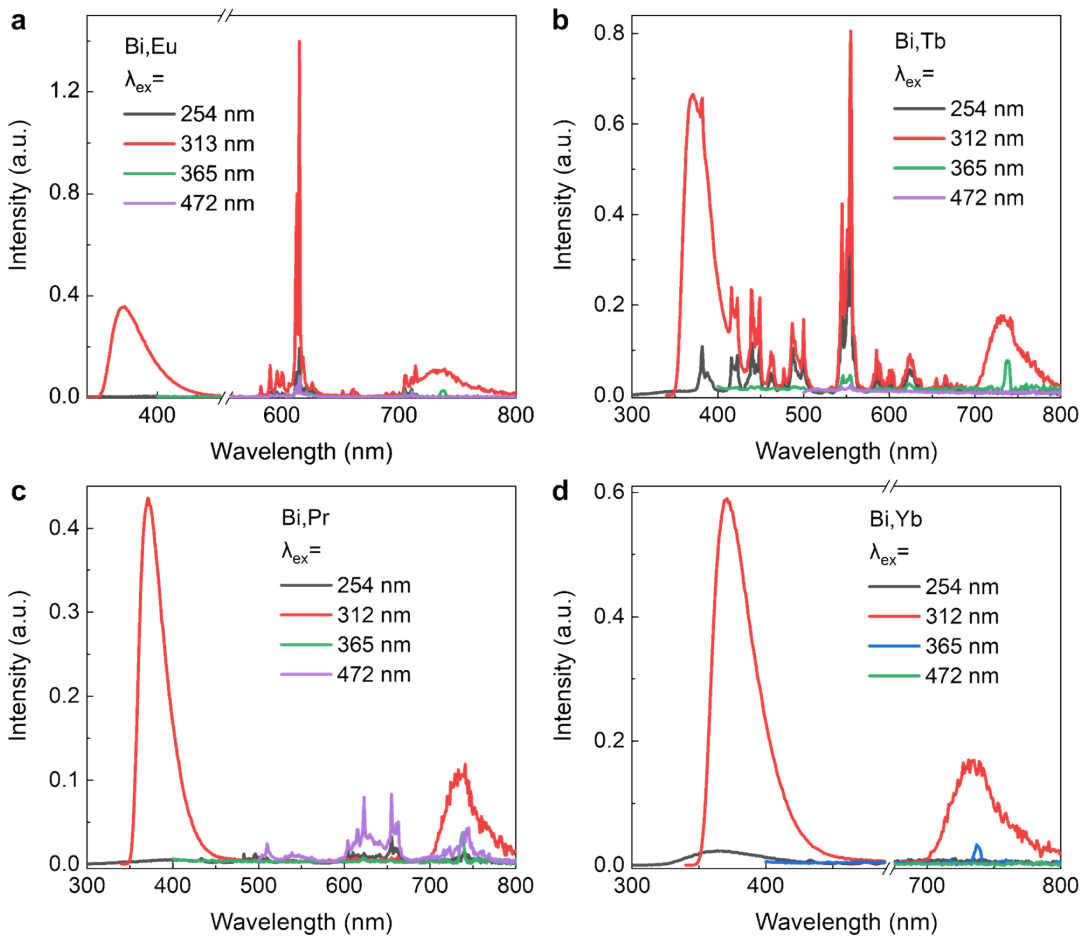

Fig. S15. Excited wavelength-dependent PL emission spectra of LLGO:Bi,Ln (Ln=Eu, Tb, Pr and Yb) phosphors. Therein, (a) LLGO:Bi,Eu, (b) LLGO:Bi,Tb, (c) LLGO:Bi,Pr, and (d) LLGO:Bi,Yb.

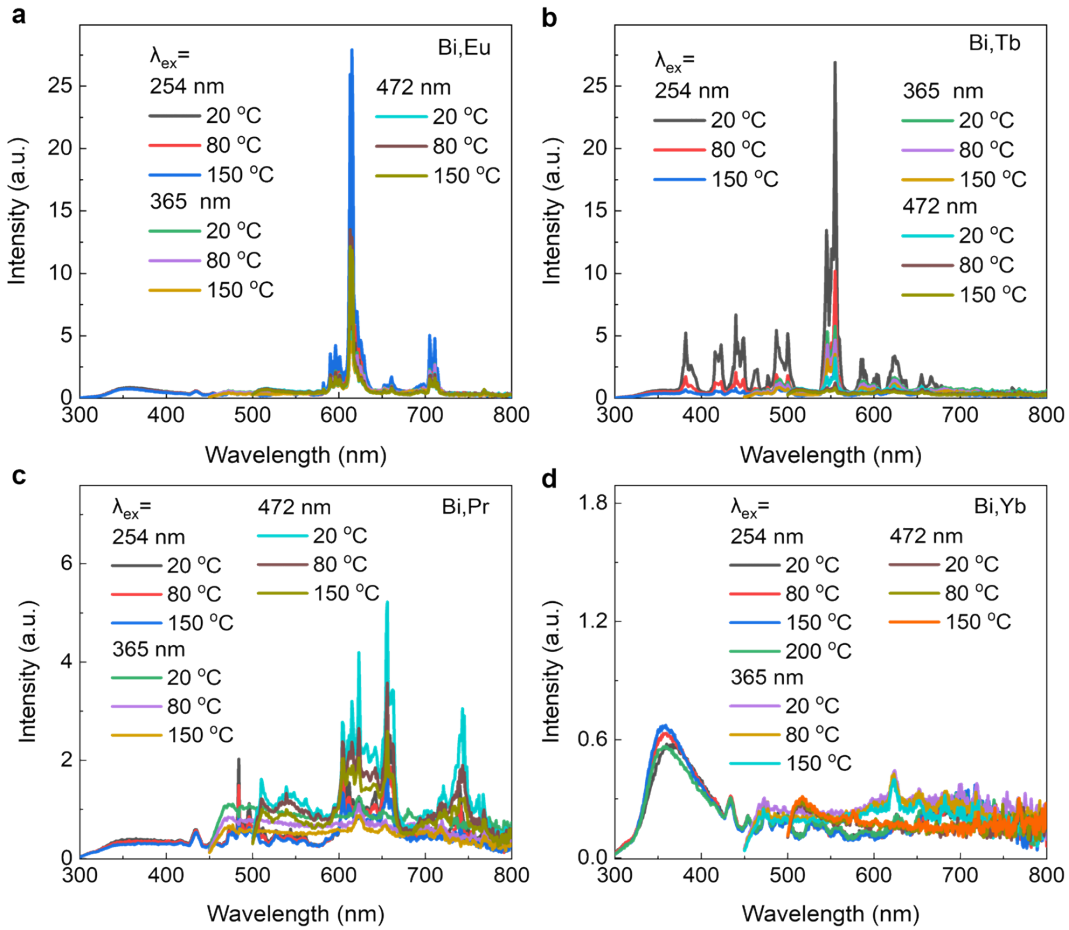

Fig. S16. Temperature-dependent PL spectra of (a) LLGO:Bi,Eu, (b) LLGO:Bi,Tb, (c) LLGO:Bi,Pr and (d) LLGO:Bi,Yb.

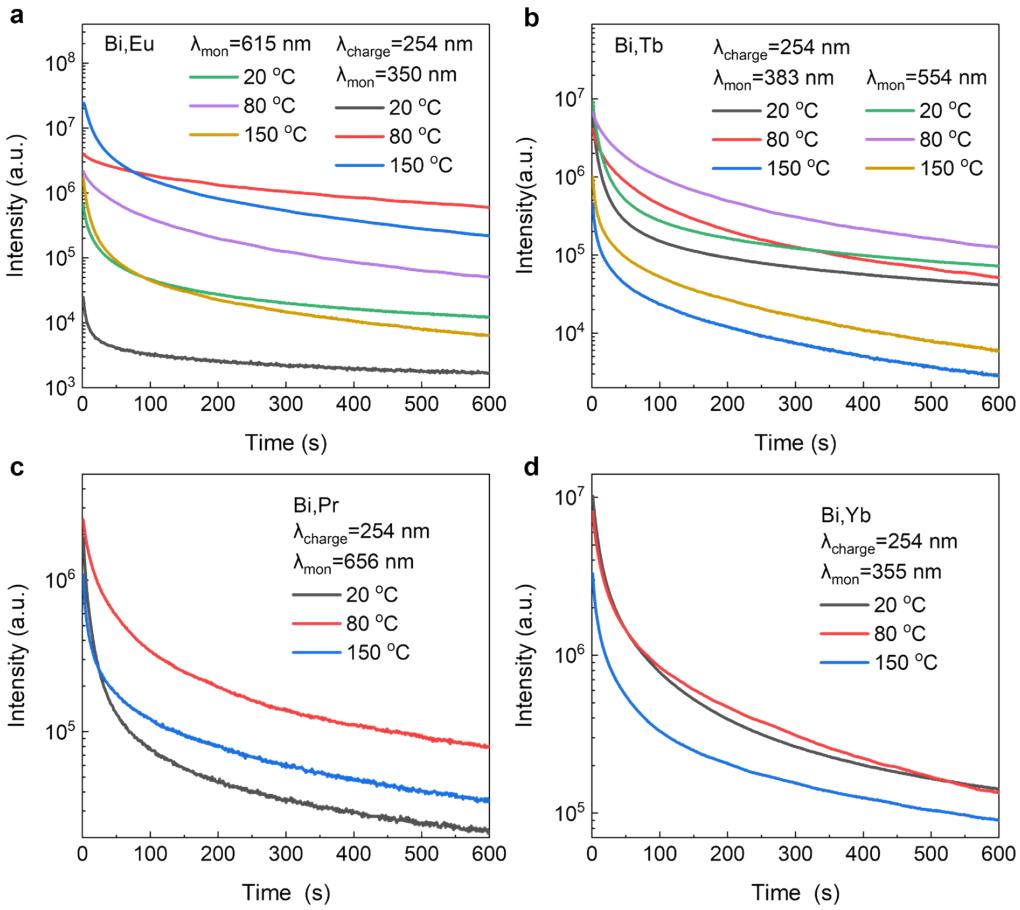

Fig. S17. Temperature-dependent PersL decay curves. (a) LLGO:Bi,Eu, (b) LLGO:Bi,Tb, (c) LLGO:Bi,Pr, and (d) LLGO:Bi,Yb. Before measuring the afterglow decay curve, the sample was pre-charged at the measurement temperature for 6 min.

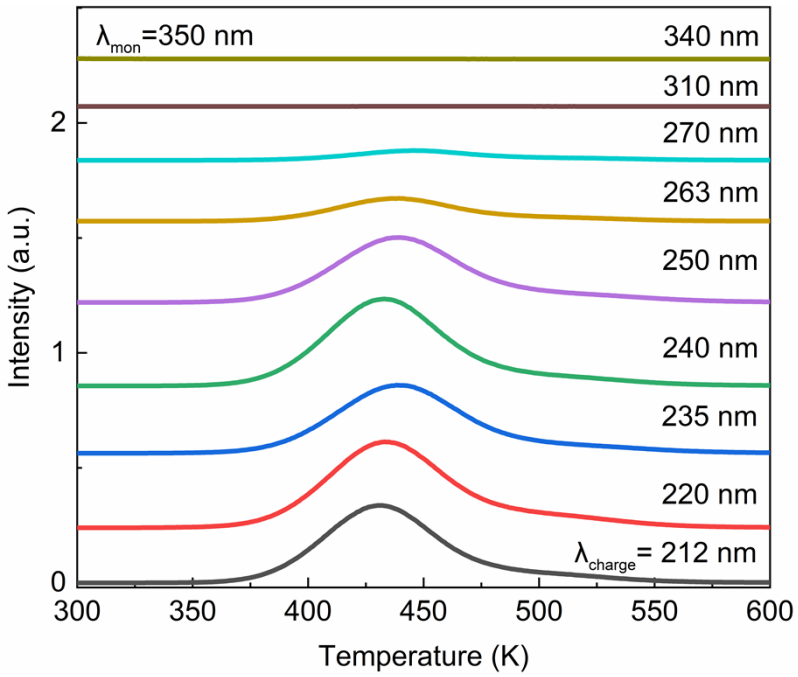

Fig. S18. Charging wavelength-dependent TL curves of LLGO:Bi, Eu phosphors.